Fatigue resistance of orthotropic steel decks

Fatigue Resistance of Orthotropic Steel Decks

Résistance à la fatigue des dalles orthotropes en acier

Dauerfestigkeit orthotroper Stahl-Fahrbahnplatten

André BIGNONNET
Engineer ENSM
IRSID
St. Germain-en-Laye, France

Bernard JACOB
Civil Engineer, IPC
LCPC
Paris, France

Jean CARRACILLI
Engineer
LCPC
Paris, France

Michel LAFRANCE
GTS TFK
Dunkerque, France

SUMMARY
The present study is a part of a large European research program dealing with the fatigue behaviour of stiffener to deck-plate welded connections. A numerical model has been developed to evaluate the durability of fatigue loaded structures. Theoretical analyses have employed fracture mechanics to describe the growth of fatigue cracks. A model has been fitted with experimental results from tests of large welded specimens which were representative of a true structure. Application of the model to existing bridges leads to prediction of fatigue damage which is in agreement with problems observed in service.

RÉSUMÉ
Cette étude réalisée dans le cadre d'un programme communautaire CECA traite du comportement en fatigue de la liaison soudée tôle de platelage-auget. Un modèle numérique de prédiction de la durabilité des structures a été développé. Il s'agit d'une analyse théorique basée sur l'approche par la mécanique de la rupture de propagation des fissures de fatigue. Le modèle a été ajusté à l'aide du travail expérimental effectué sur des éprouvettes soudées soumises à des situations de contrainte rencontrées sur les structures réelles. L'application du modèle aux cas de ponts existants a conduit à des prédictions d'endommagement par fatigue cohérentes avec des désordres observés en réalité.

ZUSAMMENFASSUNG
Diese im Rahmen eines EGKS-Programmes durchgeführte Untersuchung behandelt das Ermüdungsverhalten von geschweissten Verbindungen zwischen Belagsblech und Versteifungselement. Ein numerisches Modell für die Voraussage der Dauerfestigkeit der Strukturen wurde entwickelt. Es handelt sich um eine theoretisch-bruchmechanische Analyse der Rissausbreitung. Das Modell wurde anhand von Resultaten aus experimentellen Untersuchungen geeicht. Letztere erfolgten an geschweissten Proben, die Beanspruchungen unterworfen wurden, wie sie für wirkliche Strukturen repräsentativ sind. Die Anwendung des Modells auf existierende Brücken führte zu Vorhersagen der Beschädigung, die den tatsächlich beim Betrieb beobachteten Schäden entsprechen.

1. INTRODUCTION

The fatigue strength is an important safety criterion for the steel structures such as the orthotropic decks. For that reason the European Coal and Steel Community (ECSC) has supported a wide research program for 12 years. The last phase (1986-89) was devoted to the study of the behaviour of the most sensitive details, such as the connection between the longitudinal stiffener and the plate presented in this paper. An experimental work was conducted by the IRSID in order to establish the S-N curves adapted to the actual performant welding conditions and to provide measured lifetimes under controlled loading cases. The LCPC developed a physical model of crack propagation calculation, based on the fracture mechanics theory and implemented it to the tested specimens and to some existing bridges on which measurements were done. By this way the model calibration and validation was possible and then the results concerning the bridges were compared with those by the classical S-N approach with a Miner's summation.

2. EXPERIMENTAL WORK

2.1 Type of Connection

The work undertaken dealt with the stiffener to deck plate connection. The experimental program included two aspects :

- the optimization of the welding procedure,
- the influence of an accosting gap, 0 or 2 mm, between the stiffener and the deck plate during the welding.

The specimens whose geometry is given on figure 1 are sliced from 5.50 m long assemblies. The material used is a structural steel E 36-4 (standard NFA 501-87), TMCP steel 6 mm thick for the stiffener and normalized steel 12 mm thick for the deck plate.

2.2 Welding Operation

The stiffeners have been welded in one run in horizontal position, 2F, using a submerged arc welding automatic machine, without pre-heating nor post-heating. Filler metal and flux are of the type SAF-AS35/AS462. The influence of the edge preparation has been checked, chamfered edge at 60° or 45° and without chamfer.

The welding energy has been ajusted to minimize the lack of penetration.

From these sets of welding tests, presented in more details in reference [1] it has been shown that without edge preparation, no chamfer, a satisfactory penetration (lack of penetration $\simeq$ 1 mm) is obtained for a welding energy of 20 kJ/cm, figure 2, and this even with an accosting gap of 2 mm.

2.3 Static Tests

Tests have been performed with 3 points bending as indicated in figure 1.

For a good knowledge of the strees distribution, static tests have been done on an instrumented specimen, figure 3a. It is noted that in the median axis of the specimen the loading is biaxial with $\sigma_2/\sigma_1 = 1/3$ (σ_1 is in the direction of the bending stresses).

The nominal stresses definition to be used in the fatigue S-N diagrams are derived from these tests :

- extrapolation of the stress in the deck plate to the weld-toe, figure 3b, definition generally used when the cracks propagate through the deck plate from the weld-toe,
- extrapolation of the stress in the stiffener to the weld root, figure 3c, definition generally used when cracks propagate through the weld from the root of the weld.

2.4 Fatigue Tests

Fatigue tests have been performed in alternate bending : R=-1 ($R = S_{min}/S_{max}$).

The results are expressed in terms of the nominal stress range in the deck plate as defined above, $R = S_{max} - S_{min}$, versus the number of cycles to failure.

Two different criteria have been used in the presentation :

N_1= crack detection by extensometry, a ≃ 0.3 mm (see reference [1]).

N_4= end of test (large displacement of the actuator).

The welding procedure used leads to a lack of penetration lower than 1 mm and a throat of about 6 mm. With these conditions for R = -1, the cracks initiate systematically in the deck plate at the weld toe.

The results given in figure 4 show that for the welding conditions used there is no difference in fatigue behaviours between a stiffener welded with a gap of accosting of 2 mm and a stiffener welded without gap. The whole results with R = -1 lead to a Wöhler curve, figure 4, such as ΔS (MPa) = 26477 $N^{-1/3}$, standard deviation = 24 MPa.

On figure 5, these results are compared with those from Liège University [2] and from CRIF [3], for comparable R ratio (between -0.57 and -1) in terms of nominal stress range in the stiffener at the weld root. The primarily difference with IRSID results is that experiments of Liège University [2] and CRIF [3] show a crack initiation at the weld root, and the failure occurs in the weld. As shown in table 1, the specimen used at CRIF [3] welded by manual arc welding involve an important lack of penetration.

It is clear from figure 5 that the fatigue strength significantly increases when using submerged arc welding, this technique allows larger penetration and larger throat of the weld. Nevertheless, it is shown that cracks initiate at the weld of the root for a lack of penetration larger than 2 mm. Conversely if the welding operation is properly optimized the lack of penetration can be limited at about 1 mm and for alternate or repeated tensile bending in the deck plate the crack initiate at the weld toe, and the fatigue strength is improved. This is interesting for the purpose of inspection and structure safety. If the lack of penetration remains of the order of 1 mm, the risk of fatigue cracking is reported at the weld toe which is more accessible to control.

References	Lack of penetration (mm)	Throat (mm)
this work	1 to 1.5	5.5 to 6.5
[2]	2 to 2.5	5 to 6
[3]	3 to 4.5	3.5 to 4.5

Table 1 : Geometric welds characteristics, presented here and references

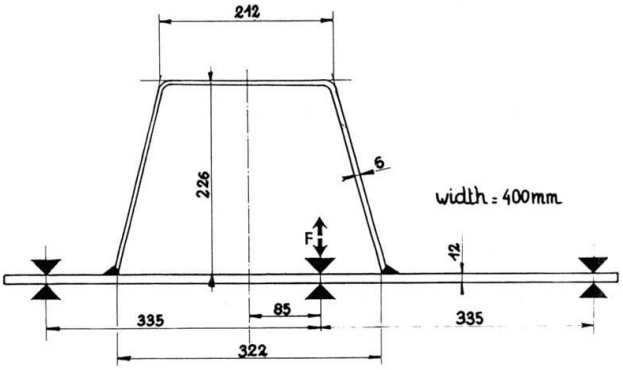

Fig.1 : Geometry of the specimen

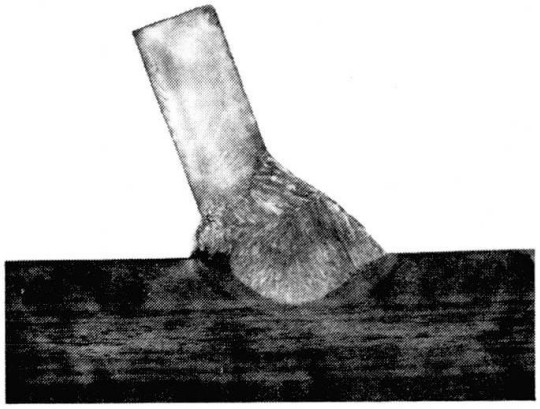

Fig.2 : Macrography of the weld

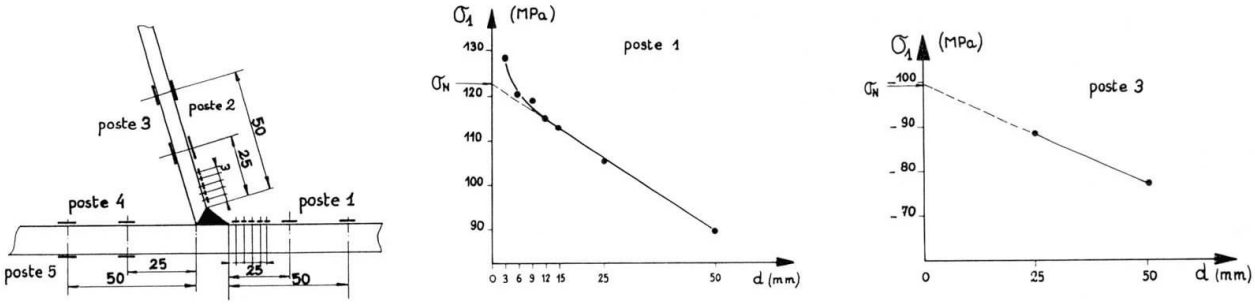

Fig.3 : Gauge instrumented specimen a), and nominal stress definition in the deck plate b) and in the stiffener c).

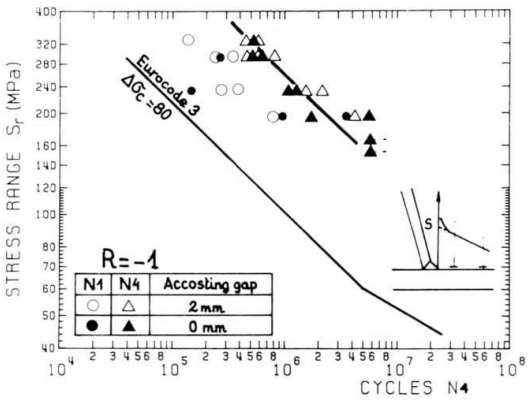

Fig.4 : Wöhler curve at R=-1 for two accosting gaps, on the basis of the stress range in the deck plate.

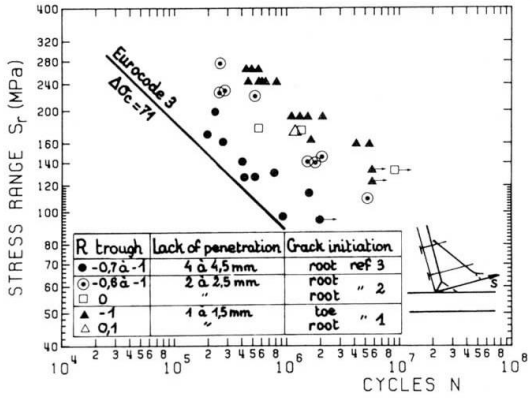

Fig.5 : Comparison of fatigue results with litterature data, on the basis of of the stress range in the stiffener.

3. FRACTURE MECHANICS ANALYSIS

3.1 Model of Damage

The classical fatigue S-N calculation with a Miner's summation, generally used by the engineers, remains the basis of most of the codes. But the strong assumptions about the linear damage accumulation, which does not take into account the stress variation time history, make this approach very poor and far from the real crack propagation phenomena.

The fracture mechanics applies the principles of the continuum mechanics to describe the crack propagation. The stress distribution is analysed in detail around the crack end. Here, only the mode I - crack opening - is considered, and the propagation time is computed. The time of crack initiation is not taken into account because it is assumed that the local surface defects already provide small cracks. This initial state is summarized by a conventionnal crack length a_0.

3.2 Propagation Law

The crack propagation is governed by the stress intensity factor K, which characterizes the local geometry of the structure and the effect of a stress variation on the crack growth rate. Between the many models proposed, we have chosen the Paris law with a threshold, one of the simplest but realistic models. The crack growth rate is given by :

$$\frac{da}{dN} = C(\Delta K - \Delta K_S)^m \qquad (1)$$

where da is the elementary increase of the crack length under dN stress variation cycles, C and m are two constant parameters which characterize the material ; ΔK_S is a threshold of non propagation. The increase of the stress intensity range under a stress variation $\Delta\sigma$ may be written :

$$\Delta K = K_M - K_m = \sqrt{\Pi a}\ \Delta\sigma\ f(a) \qquad (2)$$

where f(a) is a magnification factor representing the local geometry.

Finally, the lifetime is obtained by integration of (1) :

$$N = N_0 + \frac{1}{C}\int_{a_0}^{a_r} \Delta K^{-m}\, da \quad , \text{ where } a_r = e/2 \text{ is the failure criteria} \qquad (3)$$

e beeing the plate thickness.

3.3 Calculation of the Stress Intensity Factor

If the stress diagram $\sigma(x)$ in the non-cracked section is expressed as a polynom of x :

$$\sigma(x) = A_0 + A_1 x + A_2 x^2 + A_3 x^3 + A_4 x^4 \qquad (4)$$

then the stress intensity factor of equation (2) may be written as :

$$K = \sqrt{\Pi a}\ \left[A_0 F_0 + \frac{2a}{\Pi} A_1 F_1 + \frac{a^2}{2} A_2 F_2 + \frac{4a^3}{3\Pi} A_3 F_3 + \frac{3a^4}{8} A_4 F_4\right] \qquad (5)$$

where the F_i are the magnification factors, functions of a, the present crack length. They are calculated using a superposition principle and the successive

application of simple stress diagrams, and for a finite set of values of a. A finite element method is used in this determination. As an example, F_0 and F_1 are plotted as functions of a in the figure 6.

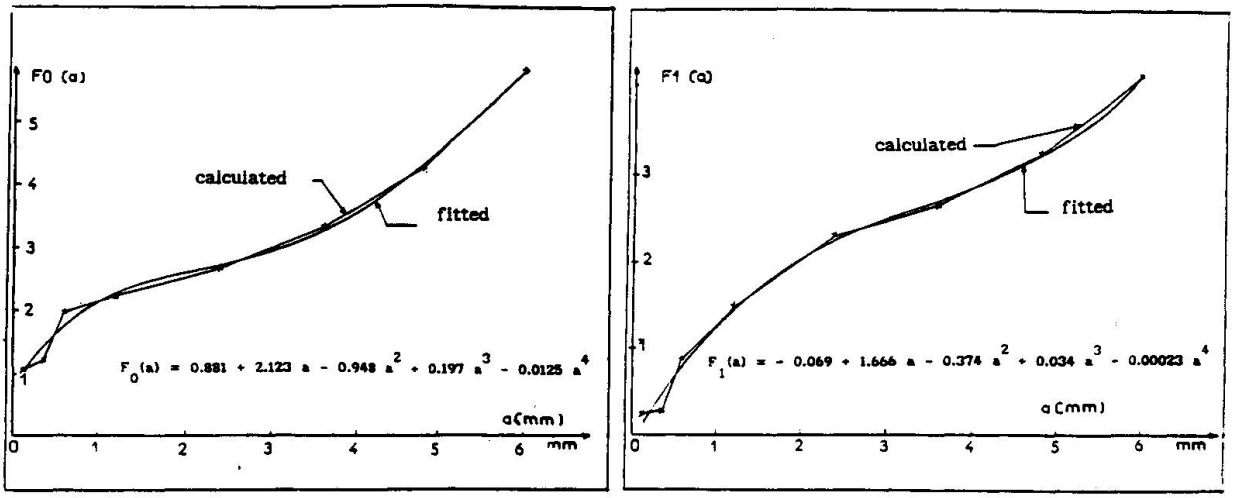

Fig. 6 Magnification factors F_0 and F_1

4. APPLICATION TO EXISTING BRIDGES

The part considered is the longitudinal welded connection between the stiffener and the plate of the orthotropic decks. It is one of the most sensitive element to fatigue damage. Several cracks have already been found in some existing bridges, especially for thin plates of 10 mm [4].

4.1 Crack Propagation Calculation

The crack is located in the plate, in a plane which is perpendicular to its surface and which contains the weld. The magnification factors are calculated as explained in the § 3-3.

The stress time history, measured by strain gauges on the bridges under a real traffic or computed by the LCPC's program CASTOR [5] by using the influence surface and a traffic record made by piezo-electric cables [6], is summarized in an histogram for a reference period T (generally T = 1 week). If N_i and N_c are the number of stress cycles with an amplitude σ_i and the total number of cycles by time unit, equations (1), (2) and (5) give :

$$da = \sum_{i=1}^{N_c} f(a,\sigma_i) N_i \, dt \quad , \text{ or } \quad da_{n+1} = \varepsilon\, a_n = \sum_{i=1}^{N_c} f(a_n,\sigma_i) N_i \, dt_{n+1} \tag{6}$$

after discretization, and with $a_r/a_0 = (1+\varepsilon)^j$; j corresponds to the total number of time steps when the failure occurs ($a = a_r$). The total lifetime is :

$$D = a_0 \sum_{k=1}^{J} \frac{\varepsilon\,(1+\varepsilon)^k}{\sum_{i=1}^{N_c} f(a_0(1+\varepsilon)^k,\sigma_i) N_i} \tag{7}$$

A computer program PROPAG [1] was written in order to compute this lifetime and to provide the crack evolution.

4.2 Model Calibration

The crack propagation calculation was first applied to the test specimens presented in the § 2, in order to calibrate some parameters and to check its results. A finite elements calculation made on the structure with the real loading and boundary conditions provided the stress diagram in the section of the plate :

$$\sigma(z) = 157.21 - 55.82\ z + 8.93\ z^2 - 0.866\ z^3 + 0.029\ z^4 \qquad (8)$$

The crack length increases were recorded during the tests for two stress amplitudes (200 and 300 MPa), and the coefficients C and m of (1) have been fitted to the results. They were found close to those proposed in the litterature and finally adopted : $C = 8.10^{-12}$, and $m = 2.85$, for ΔK in MPa $\sqrt{m}$ and da/dn in m/cycles.

In the tests we used the ratio $R = \sigma_{min}/\sigma_{max} = -1$. Because it was shown by other tests that the lifetime is highly dependent on this ratio and that only the tensile stresses allow to increase the crack, the stress amplitude taken into account here was $\sigma/2$.

The results of the calculation are compared with the experimental ones for several nominal stress from $\Delta\sigma = 200$ MPa to $\Delta\sigma = 340$ MPa, each time with 5 initial crack lengths between 0.05 mm and 0.4 mm (table 2). It is easy to conclude that an appropriate initial crack length under these welding conditions is 0.1 mm.

$R = \frac{\sigma_M}{\sigma_m}$	$\Delta\sigma$ (MPa)	Number of cycles at failure (IRSID tests)	Fracture mechanics model	
			a_0 (mm)	N. of cycles at failure
-1	200	2031000 729000 3443000 m= 2068000	0.05 0.10 0.15 0.20 0.40	3166000 1608000 1052000 777900 399900
-1	240	1076000 1274000 1767000 m= 1372000	0.05 0.10 0.15 0.20 0.40	1884000 957000 626000 463000 238000
-1	300	315000 548000 m = 431500	0.05 0.10 0.15 0.20 0.40	998000 507000 332000 245000 125900
-1	340	350000	0.05 0.10 0.15 0.20 0.40	698000 355000 232000 172000 88100

Table 2 : Comparison of the tested and computed lifetimes

4.3 Lifetimes of Existing Bridges

We present here the application of our model to the connection between the plate and the longitudinal stiffener for three cases of orthotropic deck bridges. Two of these bridges are temporary structures with a thin plate of 10 mm and a 6 mm thick stiffener (Montlhery and Choisy). The third one is the large box-girder bridge of Caronte, with a main span of 130 m and a total length of 300 m. The plate thickness is 12 mm.

In the cases of Caronte and Montlhery, the stress variations were measured under the traffic loads during previous phases of a ECSC's contract [7], by strain gauges sticked close and perpendicular to the weld. The nominal stress is obtained by a linear extrapolation, from two other points. In the case of Choisy, the stress variations are calculated by the program CASTOR, using the measured influence surface and the recorded traffic loads. The calculation is done with two traffics : the real one (RN 305) and the traffic of the RN 23 which is heavier and denser, in order to predict the consequences of an increase of the loads and traffic density.
The stress diagrams are for Montlhery and Choisy :

$$\sigma(z) = 7.533 - 2.706\ z + 0.481\ z^2 - 0.0788\ z^3 + 0.0055\ z^4 \qquad (9)$$

and for Caronte : $\sigma(z) = 6.024 - 3.287\ z + 1.075\ z^2 - 0.19\ z^3 + 0.0123\ z^4$ (9')

Due to the high residual stresses, all the stress variations under traffic loads are assumed to be in the tensile domain and hence are taken into account. The threshold of non-propagation ΔK_s has been chosen in accordance with the fatigue limit of the ECSC's S-N curves [8]. An initial crack length of 0.3 mm has been adopted corresponding to the welding conditions of these structures.

In all cases, the lifetime calculations were made by our fracture mechanics model and by the classical S-N curves and Miner's summation. The results are presented and compared in the table 3. The relevant S-N class for our element is 50 at least for the thin plates ; for Caronte the class 63 or 71 can be used. The figure 7 shows the crack evolution in the time in all cases ; a conservative choice of ΔK_s, which corresponds to the class 50, was made. This non-linear evolution is clearly different as the S-N approach. The lifetimes obtained by our model are slightly longer than those by S-N calculation, but, above all, the sensitivity to the S-N class is much lower, which seems to be more realistic.

CLASS	MONTLHERY		CARONTE		CHOISY Traffic RN 306		CHOISY Traffic RN 23	
(ECSC)	S-N	F.M.	S-N	F.M.	S-N	F.M.	S-N	F.M.
36	6	30	37	188	26	107	6	24
40	8	31	57	218	37	112	8	26
45	14	34	99	269	60	121	13	28
50	21	38	172	371	92	132	21	30
56	33	44	315	∞	138	147	31	34
63	55	55	600	∞	224	176	51	42
71	103	78	1393	∞	401	234	94	59

Table 3 : Computed lifetimes (in years) of existing bridges and comparison with S-N approach.

5. CONCLUSIONS

Two important points can be pointed out :

1/ From the manufacturing point of view it is clear that with a properly optimized automatic welding, improved fatigue resistance can be easily obtained. Therefore, taking into account the modern production tools, widely used in the european industry, it appears that the actual regulations are somewhat too conservative.

2/ From the point of view of the reliability of the structures we have shown that the physical approach of the fatigue for steel bridges can be made with a simple model which gives realistic fatigue lives, and with a lower scattering than with the classical S-N approach. The numerical program developped together with finite elements codes available, allows to make this type of calculation on a micro computer.

This study and parallel works done within the framework of the ECSC program show that the evaluation of the reliability of our bridges and the competitiveness of the steel structures still improve.

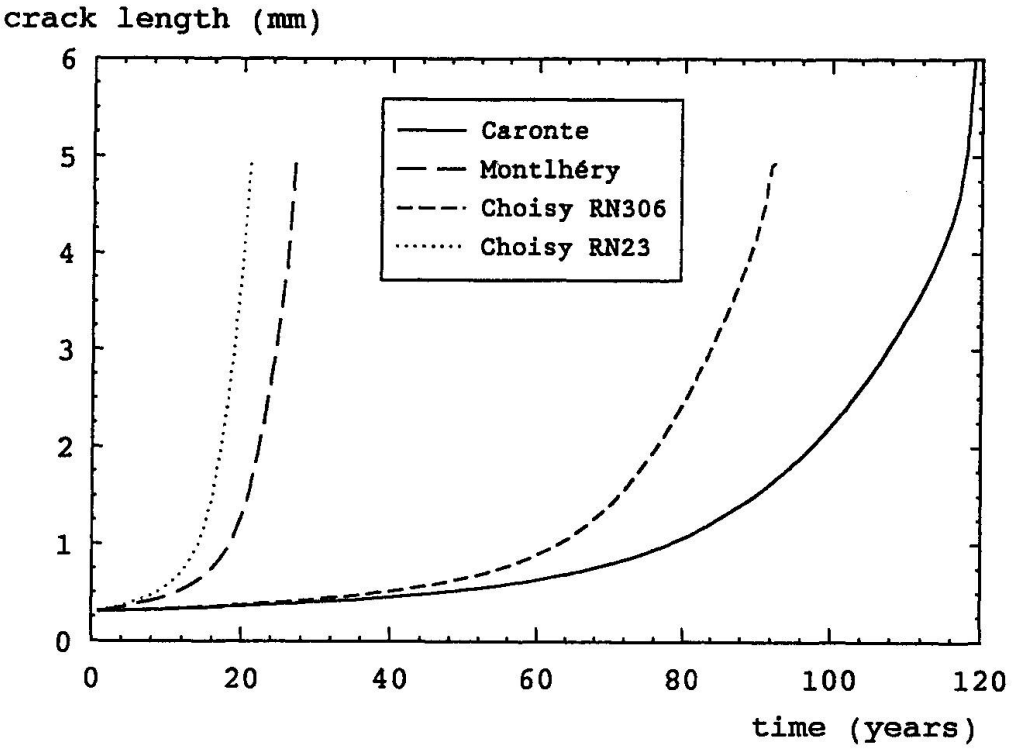

Fig. 7 : CRACK GROWTH

REFERENCES

1. BIGNONNET A., CARRACILLI J., JACOB B., Comportement en fatigue des ponts métalliques. Application aux dalles orthotropes en acier. Rapport final convention CECA, 7210 KD 217, Août 1989.

2. BRULS A., POLEUR E., Résistance à la fatigue des dalles en acier des ponts-routes. Rapport final convention CECA, KD 201, Avril 1989.

3. THONNARD, JANSS, Comportement en fatigue des dalles orthotropes avec raidisseurs trapézoïdaux. Rapport CRIF, MT 161, Août 1985.

4. MEHUE P., Fissures de fatigue dans les viaducs métalliques démontables, 13e congrès AIPC, Helsinki, juin 1988.

5. EYMARD R., JACOB B., Le programme CASTOR pour le Calcul des Actions et Sollicitations du Trafic dans les Ouvrages Routiers. Bull. liaison des LPC, n° 164, novembre-décembre 1989.

6. JACOB B., Connaissance du trafic routier et des sollicitations induites dans les ouvrages. Annales de l'ITBTP, n° 478, novembre 1989.

7. JACOB B., CARRACILLI J., Mesure et interprétation des charges dynamiques dans les ponts - Etude de la fatigue. Rapport final convention CECA, 7210 KD 311, juillet 1983.

8. Convention Européenne de la Construction Métallique, Recommandations pour la vérification en fatigue des structures en acier. Construction Métallique, n° 1 - 1987.